Towards Continuous Production of Shaped Honeycombs

Proceedings of the ASME 2018 13th International Manufacturing Science and Engineering Conference
MSEC2018
June 18-22, 2018, College Station, TX, USA

MSEC2018-6646

TOWARDS CONTINUOUS PRODUCTION OF SHAPED HONEYCOMBS

Sam E. Calisch*
Center for Bits and Atoms
Massachusetts Institute of Technology
Cambridge, Massachusetts 02139
sam.calisch@cba.mit.edu

Neil A. Gershenfeld
Center for Bits and Atoms
Massachusetts Institute of Technology
Cambridge, Massachusetts 02139
neil.gershenfeld@cba.mit.edu

ABSTRACT

Honeycomb sandwich panels are widely used for high performance parts subject to bending loads, but their manufacturing costs remain high. In particular, for parts with non-flat, non-uniform geometry, honeycombs must be machined or thermoformed with great care and expense. The ability to produce shaped honeycombs would allow sandwich panels to replace monolithic parts in a number of high performance, space-constrained applications, while also providing new areas of research for structural optimization, distributed sensing and actuation, and on-site production of infrastructure. Previous work has shown methods of directly producing shaped honeycombs by cutting and folding flat sheets of material. This research extends these methods by demonstrating work towards a continuous process for the cutting and folding steps of this process. An algorithm for producing a manufacturable cut-and-fold pattern from a three-dimensional volume is designed, and a machine for automatically performing the required cutting and parallel folding is proposed and prototyped. The accuracy of the creases placed by this machine is characterized and the impact of creasing order is demonstrated. Finally, a prototype part is produced and future work is sketched towards full process automation.

KEYWORDS

Origami, Kirigami, Honeycombs, Sandwich Panels

*Address all correspondence to this author.

INTRODUCTION

Sandwich panel construction is a ubiquitous method for supporting bending loads while minimizing weight. Stiff face sheets are bonded to a lightweight core, creating a second area moment of inertia which is significantly higher than that of the face sheets or core alone. With a robust bond and shear-resistant core, the bending loads can be transmitted into pure tension and compression of the face sheets, resulting in a very light and stiff panel. The use of such sandwich panels is limited by high production costs and a narrow range of producible geometries. This research aims to develop a continuous process for production of shaped sandwich structures which could lower production costs and open a range of transformative applications for sandwich structure technology.

Material selection methods common in mechanical design [1, 2] can be extended to sandwich panels [3]. This allows sandwich panels with varying materials and dimensions of faces and cores to be compared with monolithic panels, in terms of both performance as well as cost. As expected, this shows that sandwich panels can be made to surpass monolithic materials in bending stiffness per unit mass. More surprisingly, it is shown that in applications with at least a modest cost reduction per unit mass saved, bending stiffness per unit cost of sandwich panels can also greatly surpass that of monolithic materials. This greatly increases the applicability of sandwich panel construction from industries where performance is the primary driver of material selection to industries where cost plays a greater role. That study assumes production costs are small compared to material costs, which is true for some types of sandwich panel construction. Typically polymer foams (most often polyurethane,

polystyrene, PVC, or PMI) or lightweight woods (usually balsa or cedar) have been used as core materials in low cost applications, rather than more expensive-to-manufacture honeycomb cores. Polymer foams can be produced in a large range of densities, but their material properties are significantly less impressive than honeycomb cores. Only balsa wood rivals honeycomb cores in material properties, but the range of available densities of this wood is very limited [4]. Recent work has shown metal and composite truss cores to be an exciting new technology [5, 6, 7], but only marginal performance benefits compared to honeycomb cores have been demonstrated and significant manufacturing hurdles remain. To fully realize the benefits of replacing monolithic panels with sandwich panels, cost effective methods of manufacturing high performance honeycomb cores are required.

Production costs of honeycomb cores are high because they are conventionally produced in batch, rather than in continuous manufacturing processes [8]. Some modified geometries have been produced at scale in the packaging industry (e.g., double-walled corrugated panels), but their mechanical properties do not match those of honeycomb cores [9]. Recent work, however, has made significant progress developing novel continuous processes for honeycomb cores [10, 11], demonstrating the use of cutting and folding to cost-effectively produce honeycombs with paper and thermoplastic base materials.

These techniques demonstrate how cutting and folding processes can be effectively incorporated in continuous manufacturing, but the sandwich panels produced are all flat with uniform thickness. Flat panels with thermoplastic core and face materials can be thermoformed into curved shapes, but this is limited to nearly-flat parts with a constant thickness. Honeycombs are also sometimes machined in order to meet a prescribed shape for a sandwich panel. Besides adding to material costs, this extra manufacturing step is time consuming and requires careful process control, as the compliance of the honeycomb limits the effectiveness of chip formation [12]. Non-flat shapes may also be made by joining several independent flat panels together. These joints can be points of failure, can allow water ingress, and can offset the weight and cost savings of the honeycomb panel due to glues and fasteners.

Efficient means to produce shaped honeycombs with varying thickness would greatly increase performance and applicability of sandwich panels. For instance, a sandwich panel cross section may be varied to match the expected stresses, producing a higher performance part with lower mass and material costs. The ability to produce varied shapes also expands the applicability of sandwich panels into space-constrained applications (e.g., in the automotive industry), where flat, uniform panels can not fit around other components. Further, some applications may use the shape of a sandwich panel for a functional purpose, as in aerospace applications, where a honeycomb core can provide an aerodynamic shape to a structural part. Finally, in applications where aesthetics constrain material selection (e.g. in the furniture industry), the ability to produce shaped honeycomb panels would allow sandwich panels to replace monolithic materials, lowering material costs and mass of products.

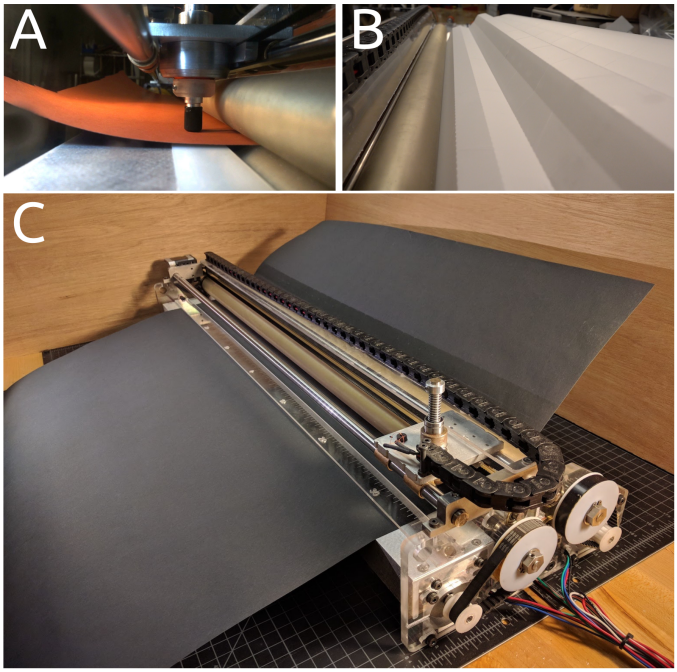

FIGURE 1. MACHINE FOR CUTTING AND FOLDING USED IN PROCESSING SHAPED HONEYCOMBS. A) VOICE COIL DRAG KNIFE CUTTING STAGE, B) CUT AND FOLDED OUTPUT FROM MACHINE, C) MACHINE PROCESSING VULCANIZED FIBER.

An approach for producing shaped honeycombs directly, requiring no post-processing operations, has come from the origami research community [13]. Similar to the continuous processes above, these techniques use *kirigami* (i.e., cutting and folding) to construct a honeycomb volume. Unlike the processes above, however, the cuts are not uniformly spaced, and their relative positions determine the three dimensional shape which is produced by folding operations. It has been shown that any constant-cross-section volume can be filled with a honeycomb produced by cutting and folding a flat sheet [14], up to a first order hold approximation at the pitch of the honeycomb. This method has been applied to airfoils [15], as well as morphing structures [16]. More recently, this technique has been extended to fill a broader class of doubly-curved three-dimensional shapes [17] by describing the folding pattern in a polar coordinate system. This opens a broader class of sandwich shapes, but has the downside that many of the folds are no longer straight and parallel, significantly increasing manufacturing complexity.

The origami research community has also produced sandwich panel cores using only folding, without any required cuts to produce honeycomb-like structures. These *foldcores* have been

the subject of considerable recent research, mostly due to their advantages for ventilating the core of a sandwich panel against water ingress [18] and high compression and shear strength [19]. Batch and continuous manufacturing processes have been demonstrated [20], but only for limited panel widths, uniform thicknesses, and with a relatively large folding pitch. There has been some work on modifying patterns of creases to create shaped foldcores [21, 22] but the patterns quickly increase in manufacturing complexity. For these reasons, this work focuses on the kirigami approaches mentioned in the previous paragraph.

The purpose of this research is to develop efficient, automated methods of producing shaped kirigami honeycombs. To date, most research has focused on developing patterns for a variety of shapes, demonstrating the methods by manual production. One recent study has shown an automated batch process for producing flat, uniform thickness kirigami honeycombs [23]. This work aims to demonstrate a continuous processes for producing shaped kirigami honeycombs. Motivated by industrial folding of maps and newspapers, we demonstrate a continuous folding machine (shown in Figure 1) capable of producing a variably spaced sequence of mountain and valley folds in a roll of material. We characterize the accuracy of this fold placement using an optical scanning technique. By adding a cutting stage on this machine, we show that two of the three required steps for producing kirigami honeycombs can be realized. Finally, we sketch a mechanism for combining the third step of the full process.

If successful, this research opens several potentially transformative capabilities beyond the simple advantages of shaped honeycombs outlined above. Similar to additive manufacturing, this process can be considered a general method to create three dimensional form. For large, lightweight parts, this method is a much more efficient means to fill space than additive manufacturing technologies. Further, it is a simple matter to cut features in the flat state to create three dimensional voids in the folded shape. This capability can be used for light-weighting, cutting away core material where it is not needed to support loads. This capability can also be used to provide channels and pass-throughs for integrating cables, hydraulic lines, and other components with the sandwich panel, rather than routing them around it. Electronics can also be efficiently placed, powered, and networked on the core material in the flat state, providing a platform for distributed sensing and actuation on the three dimensional shape.

Second, also similar to additive manufacturing, these techniques can be a viewed as a way to subvert the necessity of standardization, as the incremental cost of customization could be nearly zero. Because of this, shaped honeycombs could find applications to replace parts that are often standardized for logistical purposes. For example, large structural members like I-beams are often over specified due to standardization in manufacturing, resulting in massive unnecessary material usage [24]. Recent work [25] has demonstrated the development of a hot-rolling technique to vary the web depth of an I-beam for material efficiency, producing beams customized to their precise application requirement. A similar strategy using honeycomb cores could allow structural members to be produced with fewer limits on shape and great material efficiency.

Third, in applications where the logistics of transportation is a serious limitation on production, these techniques could enable on-site production. For instance, in the production wind turbine blades the chord length and weight of the blade creates a severe constraint for road transport due to underpass heights, telephone line heights, and subsurface conditions [26]. Shaped kirigami honeycombs could provide a way to construct large blades at the location of installation. Instead of transporting full blades, rolls of sheet materials could be easily brought to the construction site and converted on site.

Finally, as a means to specify three dimensional shape efficiently, shaped honeycombs could also find uses in applications beyond sandwich panels. One such application could be the construction of molds for concrete construction. It has been demonstrated that reductions in excess of 40% of the use of concrete in construction can be realized by carefully shaping the molds to be filled without sacrificing performance [27]. Large cell shaped honeycombs could function as molds, where the cell wall material stays in place after curing. Rebar or other reinforcement could be incorporated with the honeycomb production, providing a versatile solution for custom-shaped concrete molds, reducing the total volume used while still meeting required loads.

This paper is organized as follows: First, we detail our approach for generating cut and fold patterns for a given three-dimensional shape. It is similar, but not identical to approaches appearing in the cited literature. Next, we discuss motivation, design, and construction of the machine for folding these patterns, drawing on common mechanisms from the folding of paper media in industry. Finally, we characterize the crease spacings produced by this machine, show a shaped honeycomb produced on this machine, and sketch directions for future work.

Pattern construction

We begin by describing our method of constructing a cut and fold pattern for a honeycomb filling a three dimensional volume specified by two functions $t(x,y)$ and $u(x,y)$, which define upper and lower bounding surfaces of the volume (as shown in Figure 2). We parameterize the pitch of the desired honeycomb by its side length s and define a set of lattice coordinates

$$h(i,j) = \left(\tfrac{\sqrt{3}}{2} si, \tfrac{3}{2} s \lfloor \tfrac{j}{2} \rfloor + s(j \bmod 2) \right) \quad (1)$$

where $\lfloor x \rfloor$ denotes the smallest integer less than x and $j \bmod 2$ denotes the remainder upon division by 2. We use the shorthand $t_{i,j} = t(h(i,j))$ and $u_{i,j} = u(h(i,j))$ to denote the boundary functions evaluated at the coordinate $h(i,j)$. Figure 2 also shows a parameterized cutting and folding pattern which undergoes the transformation to become a shaped honeycomb, drawn

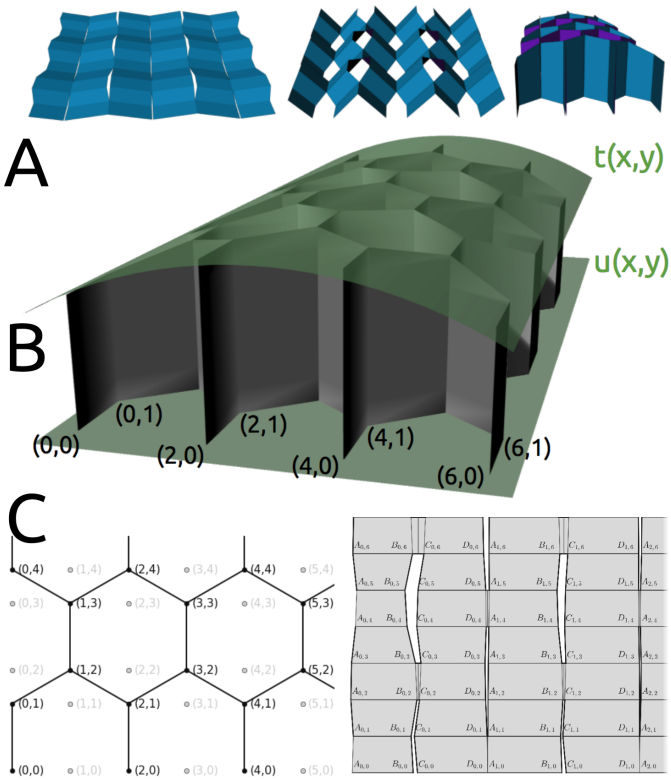

FIGURE 2. PARAMETERIZING CUT-AND-FOLD PATTERN OF A SHAPED HONEYCOMB. A) MECHANISM FOR FOLDING A FLAT PATTERN INTO A THREE-DIMENSIONAL HONEYCOMB, B) DEFINING BOUNDING SURFACES AND LATTICE COORDINATES, C) DEFINING CUT PATTERN PARAMETERS.

for the case of a regular hexagonal honeycomb. For example, after folding, the line from $A_{0,0}$ to $B_{0,0}$ runs into the page at $h(0,0)$, while the lines from $C_{0,0}$ to $D_{0,0}$ and from $A_{1,0}$ to $B_{1,0}$ run out of and into the page at $h(2,0)$, respectively. Further, the lines from $A_{0,2}$ to $B_{0,2}$ and from $C_{0,2}$ to $D_{0,2}$ run into and out of the page at $h(1,2)$, respectively. The task at hand is to choose the parameters $A_{i,j}, B_{i,j}, C_{i,j}, D_{i,j}$ such that the bounding surfaces of the resulting honeycomb match the input functions t and u.

We first note that the y coordinates in the pattern are completely determined by the lattice coordinate system and hence can be computed independently from the x coordinates. The horizontal lines are parallel and simply spaced by the side length s. Without loss of generality, we let the parameters $a_{i,j}, b_{i,j}, c_{i,j}, d_{i,j}$ denote the x coordinate of these points only. To ensure that no sections of the folding pattern overlap, we first calculate parameters $a'_{i,j}, b'_{i,j}, c'_{i,j}, d'_{i,j}$ based only on the bounding surfaces t and u. Then we calculate column-wise shifts w_i and v_i such that $a_{i,j} = a'_{i,j} + w_i$, $b_{i,j} = b'_{i,j} + w_i$, $c_{i,j} = c'_{i,j} + v_i$, and $d_{i,j} = d'_{i,j} + v_i$ determine a non-overlapping pattern.

From the correspondence between Figures 2B and 2C, we have

$$a'_{i,j} = \begin{cases} u_{2i,j} & \text{if } j \equiv 0 \text{ or } j \equiv 1 \\ u_{2i+1,j} & \text{if } j \equiv 2 \text{ or } j \equiv 3 \end{cases} \pmod 4 \tag{2}$$

$$b'_{i,j} = \begin{cases} t_{2i,j} & \text{if } j \equiv 0 \text{ or } j \equiv 1 \\ t_{2i+1,j} & \text{if } j \equiv 2 \text{ or } j \equiv 3 \end{cases} \pmod 4 \tag{3}$$

We write formulas for $c'_{i,j}$ and $d'_{i,j}$ recursively over j. Setting $c'_{i,0} = t_{2i+2,0}$, we write

$$c'_{i,j} = \begin{cases} c'_{i,j-1} - t_{2i+2,j} + t_{2i+1,j-1} & \text{if } j \equiv 0 \\ c'_{i,j-1} - t_{2i+2,j} + t_{2i+2,j-1} & \text{if } j \equiv 1 \\ c'_{i,j-1} - t_{2i+1,j} + t_{2i+2,j-1} & \text{if } j \equiv 2 \\ c'_{i,j-1} - t_{2i+1,j} + t_{2i+1,j-1} & \text{if } j \equiv 3 \end{cases} \pmod 4 \tag{4}$$

We set $d'_{i,0} = c'_{i,0} + t_{2i+2,0} - u_{2i+2,0}$ and recurse similarly over j:

$$d'_{i,j} = \begin{cases} d'_{i,j-1} - u_{2i+2,j} + u_{2i+1,j-1} & \text{if } j \equiv 0 \\ d'_{i,j-1} - u_{2i+2,j} + u_{2i+2,j-1} & \text{if } j \equiv 1 \\ d'_{i,j-1} - u_{2i+1,j} + u_{2i+2,j-1} & \text{if } j \equiv 2 \\ d'_{i,j-1} - u_{2i+1,j} + u_{2i+1,j-1} & \text{if } j \equiv 3 \end{cases} \pmod 4 \tag{5}$$

Finally, to guarantee no overlaps occur in the pattern, we set $v_0 = w_0 = 0$ and calculate recursively:

$$w_i = \max_j (d'_{i-1,j} - a'_{i,j}) + w_{i-1} \tag{6}$$

$$v_i = \max_j (b'_{i,j} - c'_{i,j}) + w_i \tag{7}$$

This parameterization is similar to that of [14], except we do not require that $d_{i,j} = a_{i+1,j}$ for $j \equiv 0, 1 \bmod 4$. and that $b_{i,j} = c_{i,j}$ for $j \equiv 2, 3 \bmod 4$. This extra freedom allows the definition of the offset parameters, which allows any bounding functions t and u to be used as bounding surfaces. This approach also maintains straight and parallel horizontal fold lines instead of using a polar coordinate system as in [17] when describing volumes with non-constant cross-section. This difference significantly simplifies the manufacturing process for these honeycombs. For instance, Figure 3 shows a wind turbine airfoil with a taper given by the optimal $1/R$ chord length scaling [28]. The bottom left image shows a fold pattern produced using a polar coordinate system to create a linearly tapering airfoil approximating the optimal scaling. The bottom right image shows a fold pattern for the optimal $1/R$ taper, produced with the current approach, keeping the folds linear, straight, and parallel. While the polar coordinate approach makes more efficient use of material, the current approach is easier to manufacture and allows greater control over shape.

The only penalty of this approach is that we must include extra pleats (e.g., $B_{0,2}C_{0,2}C_{0,3}B_{0,3}$) to account for the variable width of each column in the folding pattern. Depending on the application, these pleats can be simply trimmed off, or folded down between the adjacent honeycomb walls. In the case where

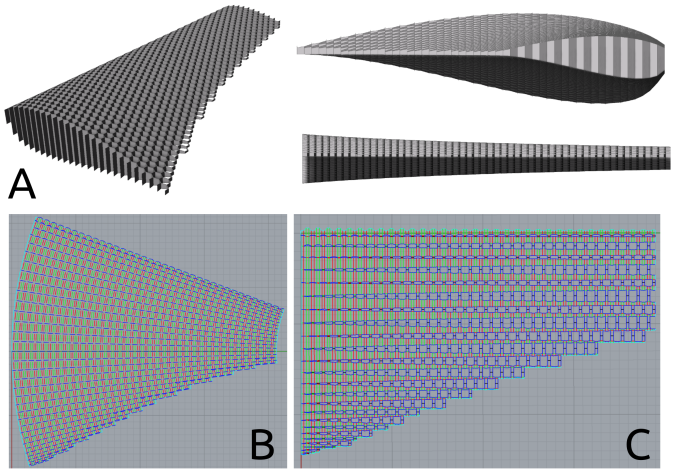

FIGURE 3. CREATING FOLDING PATTERNS FOR HONEYCOMBS WITH NON-CONSTANT CROSS SECTION. A) AIRFOIL WITH OPTIMAL 1/R CHORD LENGTH, B) LINEARLY TAPERING AIRFOIL FOLDING PATTERN IN POLAR COORDINATE SYSTEM, C) 1/R TAPERING AIRFOIL FOLDING PATTERN WITH PARALLEL CREASES AND PLEATS.

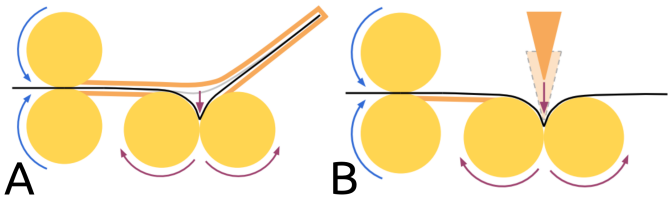

FIGURE 4. FOLDING MECHANISMS USED IN PROCESSING PRINT MEDIA. A) FOLDING USING A PHYSICAL STOP, B) FOLDING USING A MOVING KNIFE.

t and u define a volume with constant cross section (normal to y), the offset parameters equal zero. In this case, the pleats have zero size and our formulas are equivalent to those derived in [14].

Folding mechanism design

The derivation above has shown that the combination of cutting and folding operations can produce honeycombs bounded by arbitrary functions $u(x,y)$ and $t(x,y)$. For the cutting operations, there exist a large number of options for processing thin sheet materials, including passive and active knife cutting, laser cutting, abrasive waterjet machining, and die cutting. For folding, fewer options exist in industry. We now examine means to automate the required folding, developing a novel folding method capable of programmable fold spacing and orientation.

Thick or ductile materials are often folded using computer controlled press brakes or corrugation dies. Very thin materials require a small radius of curvature to reach a plastic onset strain level. Further, many papers and plastics exhibit greater elasticity than the metals which are usually folded using these methods. For these reasons, we looked to folding methods, suited to these materials and thicknesses, which correspondingly crease material to a much greater angle during forming than is required in the final, creased state. These same techniques should work on thin metal foils also, provided no brittle fracture occurs. To this end, production of maps and newspapers offers an impressive example of precise, high-speed folding at industrial scales [29]. In Figure 4, we show two folding mechanisms commonly used in this industry. In both cases, a set of rollers at the left pulls a sheet into the machine where it is folded. In the left configuration, a physical stop is positioned so that a moving sheet hits it, forming a buckle. Guides support the paper everywhere except the desired location for the buckle. This buckle is then grabbed and creased by a set of folding rollers. The process at the right is similar but uses a descending knife to push a buckle into the set of folding rollers. The position of the buckle on the sheet is set not by the physical position of a stop, but by the timing of the knife's movement relative to the moving sheet. In this way, fold position on the sheet can be varied in real time, unlike as with the first mechanism. The price to this functionality an additional degree of freedom as compared to the first mechanism.

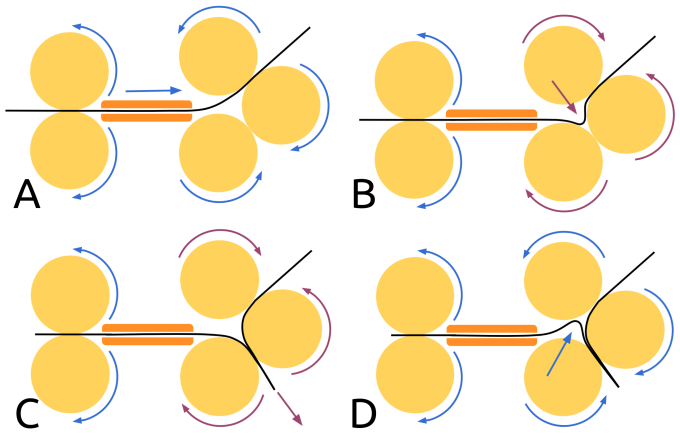

FIGURE 5. NOVEL MECHANISM FOR PROGRAMMABLE FOLDING WITH ARBITRARY FOLD SPACING AND ORIENTATION. A-D) PERFORMING A MOVE SEQUENCE TO CREATE A VALLEY-MOUNTAIN FOLDING PATTERN.

To produce a set of folds, multiple versions of these mechanisms are connected in series; as a sheet travels from one to the next, a desired set of folds is produced. As the honeycomb folding patterns derived in the last section contain a large number of parallel folds, it is untenable to have such a large number of independent folding mechanisms. Further, as drawn, both mech-

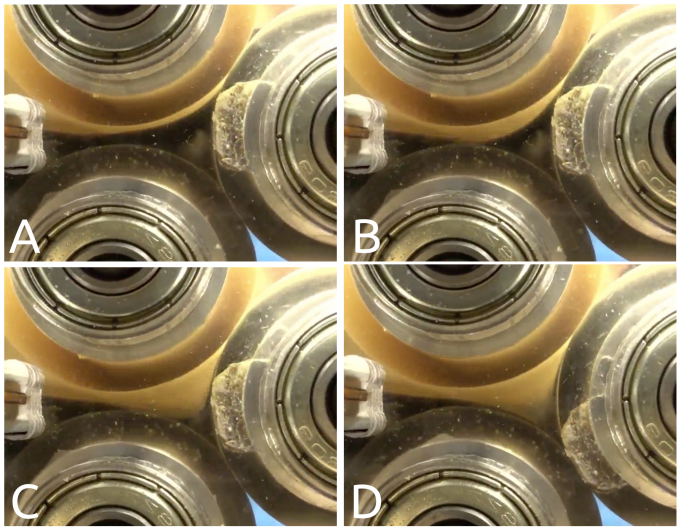

FIGURE 6. FORMING A FOLD INSIDE THE MACHINE. A) SHEET TRAVELING THROUGH ROLLERS, B) REAR ROLLER REVERSES DIRECTION, CAUSING BUCKLE TO FORM, C) CURVATURE OF BUCKLING INCREASES, D) CREASE IS FORMED AS THE BUCKLE PASSES BETWEEN ROLLERS.

anisms are only capable of producing upwards facing "valley" folds. If a downwards facing "mountain" fold is desired, inverted versions of the mechanisms are required.

Based on these constraints, we designed a novel mechanism (shown in Figure 5) inspired by the preceding two which is capable of forming both mountain and valley folds at locations which can be varied in real time, using only two degrees of freedom. To see this, consider the top left image where material enters through a roller at the left and exits through a roller at the top right. If these two rollers turn in the same orientation, the sheet simply moves through the machine. If they turn in opposite directions, a buckle is formed and folded by the third pair of rollers (shown at top right and bottom left). In this way, we have used the top right roller as a programmable stop, allowing us to place a valley fold at a variable position on the sheet. The symmetry of this configuration, however, also allows us to create mountain folds, provided we have first pulled the sheet into the bottom roller pair (shown at bottom right). The progressive formation of a buckle and then a fold is shown in Figure 6.

In fact, this mechanism is universal, in that it can fold any sequence of mountain and valley folds, provided the sequence starts with a valley, and the minimum crease spacing is lower bounded by a constant ε, depending on the machine dimensions. In practice, the first condition is not a significant constraint, as we can always perform a valley fold at the start of operation, discarding the valley after all folding has been performed. The second condition is a harder constraint, as if crease spacing is

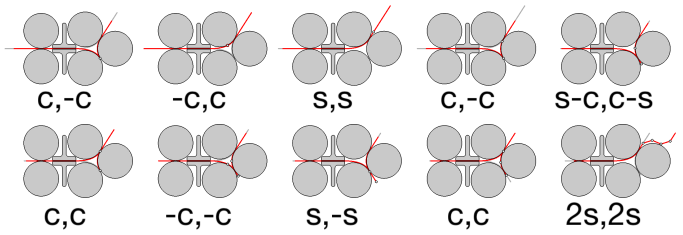

FIGURE 7. A MOVE SEQUENCE TO CREATE A V-V-M-M FOLD SEQUENCE BY FOLDING CREASES IN ORDER.

less than the distance between the contact points of the folding roller pairs, consecutive creases can interact inside the machine. In practice, the exact value of ε depends on the orientation of the incident creases. If they have opposite orientation (one a valley and one a mountain), ε was determined experimentally to be roughly $d/3$, where d is the diameter of the rollers. If the incident creases have the same orientation (both valleys or both mountains), dense crease spacing presented few problems, and hence ε was considerably smaller than in the first case.

Given a particular pattern of creases to form with this machine, we must generate a set of commands to send to the motors driving the rollers. In the case of producing honeycomb cores, we must produce a repeating valley-valley-mountain-mountain pattern with a constant spacing s. In Figure 7 we show a simple command set which produces this folding pattern where each command consists of the distance to drive each degree of freedom in the machine. In this commands, the variable c is a distance we drive both roller pairs to transform an initially taut sheet into a buckled, then creased state (the transition shown in Figure 6). We can choose any value for c as long as it is greater than $\pi d/12$, the approximate minimum distance to drive the midpoint of the taut sheet to the point of mutual tangency of the opposing rollers. In this figure, we first crease and uncrease a valley fold, then advance by the crease spacing before creasing another valley fold. With this valley fold held, we drive to the location of the subsequent mountain fold before creasing and uncreasing it. Finally, we drive to the location of the final mountain fold, crease it, and then eject all the folds from the machine.

Figure 8 shows another command set which produces the same folding pattern. In contrast to the previous command set, these folds are not produced in a consecutive order. The advantage of this pattern is that the minimum distance during folding between folds of opposite orientation is $2s$, rather than s. For dense spacings, where $s < \varepsilon < 2s$, this nonconsecutive sequence can be folded accurately, while the consecutive pattern cannot. This is measured empirically in the Results section.

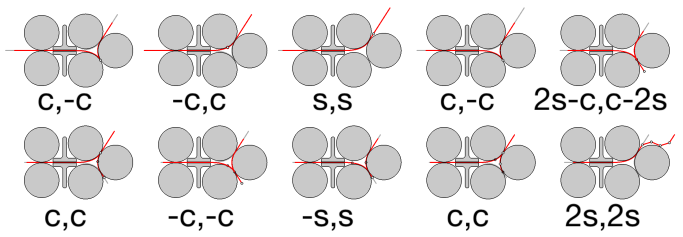

FIGURE 8. A MOVE SEQUENCE TO CREATE A V-V-M-M FOLD SEQUENCE BY FOLDING CREASES OUT OF ORDER.

Machine construction

To construct the folding machine, a set of pinch rollers were fabricated by overmolding Shore 80A urethane rubber (Smooth-On PMC-780 Dry) onto 25 mm aluminum rods. The rubber was pressure cast, demolded, rough turned, and finished ground, as shown in Figure 9. Two grit rollers were fabricated by knurling an aluminum rod of the same diameter as the urethane pinch rollers. All rollers had an outer diameter of 32 mm and were sized to give a 750 mm working width for the machine.

In selecting these dimensions, we sought a balance between the maximum width material capable of being processed and the densest crease spacing possible. The wider the input material, the larger, thicker the honeycombs that can be produced. Over a large width, however, deflection of the rollers would decrease the effectiveness of the machine's creasing operation. We expected that increasing the roller diameter to compensate for this would limit the minimum spacing of creases that the machine would be capable of producing. Therefore, to balance these competing design constraints, we sized the rollers based on the expected forces per unit length required to form a plastic hinge in the material. It has been shown [30] that under a creasing force, the ratio of radius of curvature to the material thickness initially follows a plastic deformation power law. At some point, a discontinuity occurs, and additional force produces much smaller changes in residual curvature. For Tyvek of 143 micron thickness, this discontinuity was experimentally shown to occur at 200 N/m at a radius of curvature of 750 microns, while increasing the force per unit length to 1000 N/m only reduced the radius of curvature to 500 microns. Approximating the rollers as uniformly loaded beams with circular cross section, we can calculate the maximum deflection of the center point subject to these creasing loads. We can then calculate the maximum width subject to a deflection equal to the radius of curvature of the crease. Using this approach, we calculated that aluminum rollers of 25 mm diameter at 750 mm length would be able to crease this Tyvek. Given that Tyvek is a very elastic material requiring high force to induce crisp fold, we reasoned that more plastic materials would be creasable with rollers of these dimensions.

These rollers were arranged into a front pair of driving rollers and a rear triple of folding rollers. The rotation of these roller groups was synchronized using spur gears and actuated using a pair of NEMA-23 bipolar stepper motors and a 3:1 timing belt reduction. These motors have 200 steps per revolution, giving a potential resolution of roughly 160 microns without microstepping, or 20 microns with 1/8th microstepping.

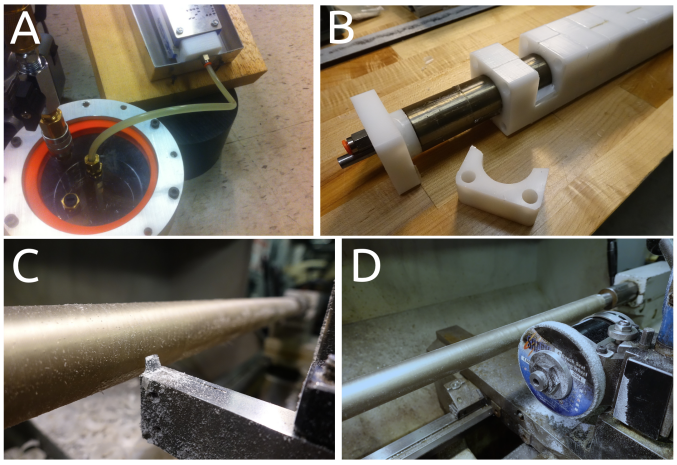

FIGURE 9. FABRICATION OF ROLLERS USED IN THE FOLDING MACHINE. A) PRESSURE MOLDING OF POLYURETHANE RUBBER ONTO ALUMINUM ROD, B) DEMOLDING ROLLER, C) ROUGH TURNING POLYURETHANE SURFACE USING HIGH RAKE TOOL, D) FINISH GRINDING SURFACE TO DIMENSION.

The cutting stage was built around a Roland drag knife holder (XD-CH2) using a 3D printed voice coil bobbin wound with 400 turns of 30 AWG magnet wire, rare earth magnets inside a 12L14 steel enclosure, and an LM8UU linear bearing with return spring. This simple voice coil actuator produced roughly 300 grams of downward cutting force, more than enough to cut a variety of sheet stocks up to 500 micron thickness.

When the sheet emerges from the machine, it has been cut according to the pattern, and the majority of creases have been folded. We call these straight and parallel folds spanning the entire pattern the corrugation folds. The remaining folds, which we call the zig-zag folds, transform the corrugated sheet into a honeycomb core. At this stage, some process for cross linking adjacent walls is necessary to retain the honeycomb in a condensed state. In the case of sandwich panels, this usually involves bonding face sheets to the core. In Figure 11, we bond cell walls with adhesive to avoid the need for face sheets. The machine presented above can automate the cutting and corrugation folding, but it doesn't yet automate the zig-zag folding. Later, we sketch an extension for automating the complete process.

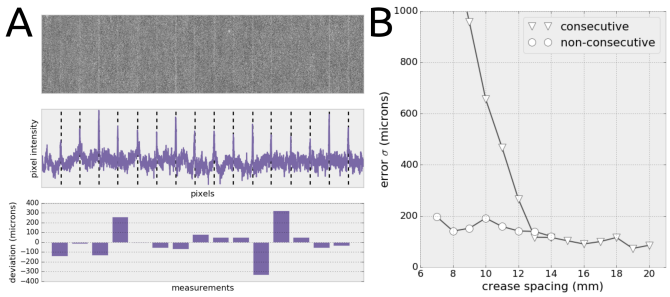

FIGURE 10. WORKFLOW FOR MEASURING ACCURACY OF MACHINE-PLACED CREASES. A) MEASURING CREASE LINES FOR 9MM SPACING SHOWING SCANNED IMAGE, DETECTED CREASES, AND PLOTTED ERRORS, B) PLOTTING ERRORS VS. CREASE SPACING FOR CONSECUTIVE AND NON-CONSECUTIVE MOVE STRATEGIES.

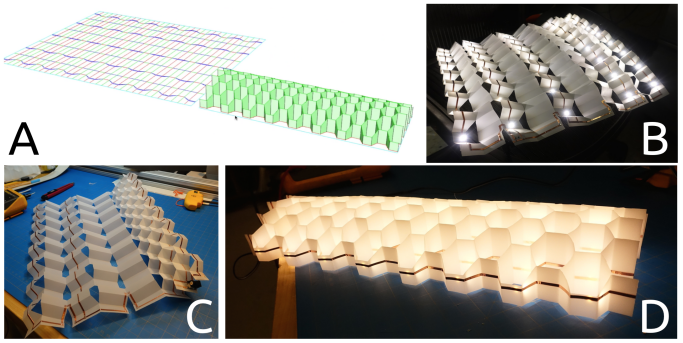

FIGURE 11. A PROTOTYPE FABRICATED USING FOLDING MACHINE. A) DIGITAL DESIGN OF 3D FORM AND 2D PATTERN, B) AFTER MACHINE PROCESSING, C) DURING FACE BONDING, D) COMPLETED PROTOTYPE.

RESULTS

Crease spacing evaluation

To characterize the accuracy of creasing using this folding method, a simple experiment was constructed. Vulcanized fiber sheets of 125 micron thickness were prepared. These sheets crease consistently and exhibit strain whitening of the crease lines. This allows optical measurement of the spacing of crease lines. The folding machine was used to crease the sheets in a repeating valley-valley-mountain-mountain pattern, with trials for many values of the desired crease spacing (from 7 mm to 20 mm). The sheets were flattened and scanned at a resolution of 100 dots per millimeter using an Epson Perfection V19 photo scanner. These images were processed using a Python script with the Numpy and OpenCV [31] libraries to detect the crease lines.

The results of this experiment are shown in Figure 10. At the left, we show the results from a particular trial where the desired spacing was 9 mm. The top image shows the scanned sample, the middle image shows the measured intensity values and detected peaks, and the bottom graph plots the difference between spacing of each consecutive pair and the desired value of 9 mm. The graph at right shows results over all crease spacings.

For crease spacings larger than 12 mm, a consecutive strategy for folding the creases produces errors with a standard deviation of roughly 100 microns. Below this spacing, however, the densely spaced creases can interfere with each other during folding. In this case, folding the creases out of order can avoid collisions. In the case of a repeated valley-valley-mountain-mountain pattern, folding in the order 1-2-4-3 eliminates a collision between the third crease and one of the rollers. Using this non-consecutive sequence, we can produce the same pattern down to 7 mm crease spacing with standard deviation of error below 200 microns. The move sequences for these consecutive and non-consecutive strategies are shown in Figures 7 and 8, respectively.

Prototypes

In order to test the built machine, we designed and fabricated a simple shaped honeycomb using PETE film (130 micron thickness). As shown in Fig. 11 at top left, the shape was designed to be flat on one side and parabolic on the other based on a honeycomb with s =7.5mm. In the top right image, the sample is shown after being processing by the machine, and after initial zig-zag folding has been performed manually. At bottom left, the sample is shown during bonding of adjacent faces. At bottom right, the finished sample is shown.

This sample was also used to show the viability of combining this manufacturing process with the production of flexible printed circuit boards. The shaped honeycomb acts as a carrier for an array of LEDs, positioning them accurately in three dimensional space based on their placement on the two dimensional material. The copper traces are applied using a pressure set adhesive after leaving the folding machine, but more common etching processes could be used prior to folding as well.

FUTURE WORK

This research opens several directions for future work. First, full process automation for shaped honeycombs requires the addition of a final stage of this continuous process where the cut and corrugated sheet is folded in a zig-zag fashion into the final honeycomb. Depending on the application, this stage of the process may take different forms, but in the case of sandwich panels it involves gathering the cut and corrugated output from the folding machine into a honeycomb form and attaching face sheets. Similar “pattern and gather” approaches have experienced considerable success [32] in efforts to automate the folding of other origami patterns. In these techniques, a sheet is weakened along crease lines by partial cutting operations and a global contraction can cause all the creases to be folded synchronously. A sketch of

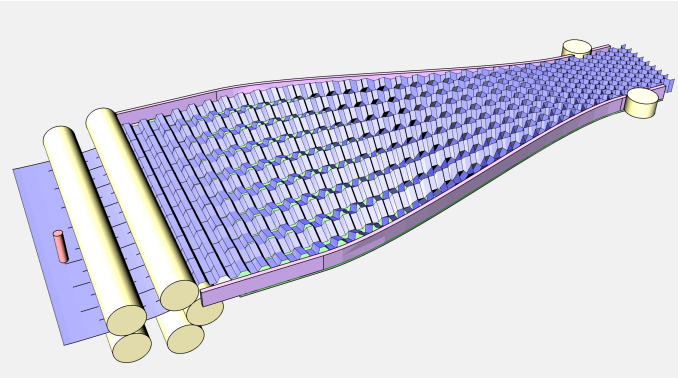

FIGURE 12. CONCEPT FOR GATHERING FOLDING MACHINE OUTPUT INTO A HONEYCOMB SANDWICH PANEL.

this technique as applied to the shaped honeycomb problem is shown in Figure 12. The machine detailed above feeds its output into a narrowing passage, finally passing through its minimum width with the assistance of pulling rollers. Once started, each column of honeycomb cells imparts a bias to the next column of cells, extending the zig-zag fold. The corrugation makes each row stiff in comparison to the zig-zag crease lines, increasing the effectiveness of the gathering process. Once gathered, face sheets can be applied to fix the honeycomb in its condensed state.

A second direction for future work is to fully exploit the ability of the machine presented in this research to produce honeycomb cores of continuously varying cell size. This can be easily accomplished by changing the honeycomb cell side length s by placing corrugation folds at a different spacing. This capability could be used to provide a dense, stiff core in a region that experiences high loads (e.g., at the root of a wind turbine blade), while placing a much lighter core in regions (e.g., at the tip of the wind turbine blade) where high load capacity is not needed and weight savings has significant benefit.

A third direction for future work is to develop manufacturing processes for folding patterns closely related to hexagonal honeycombs which use additional folds to create a mechanism allowing the cells to change in height [33, 34, 35]. These mechanisms can tune the elastic modulus of a honeycomb for applications which require compliance instead of maximized stiffness.

Finally, an especially compelling direction for future work is building functional honeycomb cores using the construction presented as a way to address three dimensional space based on the location of elements on a two dimensional sheet. A simple example was presented using surface mount LEDs, but the same idea can be extended to a broad range of distributed sensing and actuation technologies. For instance, strain gauges can be used to monitor loads applied to the sandwich panel, conductive elements can turn the honeycomb core into a communications antenna, or electromagnetic actuators could produce a movement of the sandwich skin or panel itself.

CONCLUSION

This research has shown work towards continuous manufacturing of shaped honeycombs. First, an algorithm for computing flat patterns of cuts and folds based on three dimensional geometry was developed. Based on the large proportion of straight and parallel folds produced in these patterns, a machine was designed to both produce these folds as well as make the required cuts.

This machine was then characterized by measuring the deviation of the placed folds from the desired fold locations. It was shown that with appropriate choice of crease order, the error can be kept below 200 microns over a range of desired crease spacings of 7 to 20 mm. A simple prototype was produced with this machine demonstrating its ability to combine cutting and folding to create a shaped honeycomb. Finally, several exciting directions for future work were identified.

ACKNOWLEDGMENT

This work was supported by the Center for Bits and Atoms Research Consortia.

REFERENCES

[1] Ashby, M., 2000. "Multi-objective optimization in material design and selection". *Acta Materialia,* ***48***(1), pp. 359 – 369.

[2] Ashby, M., 1991. "Overview no. 92: Materials and shape". *Acta Metallurgica et Materialia,* ***39***(6), pp. 1025 – 1039.

[3] Pflug, J., Vangrimde, B., and Verpoest, I., 2003. "Material efficiency and cost effectiveness of sandwich materials". In INTERNATIONAL SAMPE SYMPOSIUM AND EXHIBITION, SAMPE; 1999, pp. 1925–1937.

[4] Cripps, D., 2017. Core materials. `https://netcomposites.com/guide-tools/guide/core-materials`.

[5] Sypeck, D. J., 2005. "Cellular truss core sandwich structures". *Applied Composite Materials,* ***12***(3), pp. 229–246.

[6] Wicks, N., and Hutchinson, J. W., 2001. "Optimal truss plates". *International Journal of Solids and Structures,* ***38***(30), pp. 5165–5183.

[7] Wang, B., Wu, L., Ma, L., Sun, Y., and Du, S., 2010. "Mechanical behavior of the sandwich structures with carbon fiber-reinforced pyramidal lattice truss core". *Materials and Design (1980-2015),* ***31***(5), pp. 2659 – 2663.

[8] Pflug, J., Vangrimde, B., Verpoest, I., Bratfisch, P., and Vandepitte, D., 2003. "Honeycomb core materials: New concepts for continuous production of honeycomb core materials". *Sampe journal,* ***39***(6), pp. 22–30.

[9] Pflug, J., Verpoest, I., Bratfisch, P., and Vandepitte, D., 2001. "Thermoplastic folded honeycomb cores–cost efficient production of all thermoplastic sandwich panels". *KU Leuven, Dept. Mechanical Engineering,(no date)*.

[10] Pflug, J., Vangrimde, B., Verpoest, I., Vandepitte, D., Britzke, M., and Wagenführ, A., 2004. "Continuously produced paper honeycomb sandwich panels for furniture applications". In 5th Global Wood and Natural Fibre Composites Symposium. Kassel, Germany, April, pp. 27–28.

[11] Bratfisch, J. P., Vandepitte, D., Pflug, J., and Verpoest, I., 2005. "Development and validation of a continuous production concept for thermoplastic honeycomb". In *Sandwich structures 7: advancing with sandwich structures and materials*. Springer, pp. 763–772.

[12] Qiu, K., Ming, W., Shen, L., An, Q., and Chen, M., 2017. "Study on the cutting force in machining of aluminum honeycomb core material". *Composite Structures,* ***164***(Supplement C), pp. 58 – 67.

[13] Nojima, T., and Saito, K., 2006. "Development of newly designed ultra-light core structures". *JSME International Journal Series A Solid Mechanics and Material Engineering,* ***49***(1), pp. 38–42.

[14] Saito, K., Pellegrino, S., and Nojima, T., 2014. "Manufacture of arbitrary cross-section composite honeycomb cores based on origami techniques". *Journal of Mechanical Design,* ***136***(5), p. 051011.

[15] Saito, K., Agnese, F., and Scarpa, F., 2011. "A cellular kirigami morphing wingbox concept". *Journal of intelligent material systems and structures,* ***22***(9), pp. 935–944.

[16] Neville, R. M., and Scarpa, F., 2015. "Design of shape morphing cellular structures and their actuation methods". In ICAST2015: 26th International Conference on Adaptive Structures and Technologies, Kobe, Japan. doi, Vol. 10.

[17] Saito, K., Fujimoto, A., and Okabe, Y., 2016. "Design of a 3d wing honeycomb core based on origami techniques". pp. V05BT07A026–.

[18] Klett, Y., and Drechsler, K., 2011. "Designing technical tessellations". *Origami,* ***5***, pp. 305–322.

[19] Heimbs, S., 2013. "Foldcore sandwich structures and their impact behaviour: an overview". In *Dynamic failure of composite and sandwich structures*. Springer, pp. 491–544.

[20] Elsayed, E., and Basily, B. B., 2004. "A continuous folding process for sheet materials". *International Journal of Materials and Product Technology,* ***21***(1-3), pp. 217–238.

[21] Hahnel, F., Wolf, K., Hauffe, A., Alekseev, K. A., and Zakirov, I. M., 2011. "Wedge-shaped folded sandwich cores for aircraft applications: from design and manufacturing process to experimental structure validation". *CEAS Aeronautical Journal,* ***2***(1), pp. 203–212.

[22] Klett, Y., 2013. "Realtime rigid folding algorithm for quadrilateral-based 1-dof tessellations". pp. V06BT07A031–.

[23] Wang, L., Saito, K., Gotou, Y., and Okabe, Y., 2017. "Design and fabrication of aluminum honeycomb structures based on origami technology". *Journal of Sandwich Structures & Materials,* ***0***(0), p. 1099636217714646.

[24] Allwood, J. M., Cullen, J. M., Carruth, M. A., Cooper, D. R., McBrien, M., Milford, R. L., Moynihan, M. C., and Patel, A. C., 2012. *Sustainable materials: with both eyes open*. UIT Cambridge Cambridge.

[25] Carruth, M. A., and Allwood, J. M., 2012. "The development of a hot rolling process for variable cross-section i-beams". *Journal of materials processing technology,* ***212***(8), pp. 1640–1653.

[26] Composites, T., 2003. "Cost study for large wind turbine blades: Windpact blade system design studies, sand2003-1428". *Albuquerque, NM: Sandia National Laboratories*.

[27] Orr, J. J., Darby, A. P., Ibell, T. J., Evernden, M., and Otlet, M., 2011. "Concrete structures using fabric formwork". *The Structural Engineer,* ***89***(8), pp. 20–26.

[28] Manwell, J. F., McGowan, J. G., and Rogers, A. L., 2010. *Wind energy explained: theory, design and application*. John Wiley & Sons.

[29] Mertens, K., 2001. Folding and scoring: Finishing of coated papers after sheet-fed offset printing. Tech. rep., Sappi.

[30] Rao, A., Tawfick, S., Shlian, M., and Hart, A. J., 2013. "Fold mechanics of natural and synthetic origami papers". In ASME 2013 International Design Engineering Technical Conferences and Computers and Information in Engineering Conference, American Society of Mechanical Engineers, pp. V06BT07A049–V06BT07A049.

[31] OpenCV, 2017. Open source computer vision library. `https://github.com/opencv/opencv`.

[32] Schenk, M., 2012. "Folded shell structures". PhD thesis, University of Cambridge.

[33] Cheung, K. C., Tachi, T., Calisch, S., and Miura, K., 2014. "Origami interleaved tube cellular materials". *Smart Materials and Structures,* ***23***(9), p. 094012.

[34] Tachi, T., and Miura, K., 2012. "Rigid-foldable cylinders and cells". *J. Int. Assoc. Shell Spat. Struct,* ***53***(4), pp. 217–226.

[35] Miura, K., and Tachi, T., 2010. "Synthesis of rigid-foldable cylindrical polyhedral". *Symmetry: Art and Science, International Society for the Interdisciplinary Study of Symmetry, Gmuend*.